ACS APPLIED MATERIALS & INTERFACES

Research Article

www.acsami.org

Permanent Flame Retardant Finishing of Textiles by Allyl-Functionalized Polyphosphazenes

Thomas Mayer-Gall,[†,‡] Dierk Knittel,[†] Jochen S. Gutmann,[†,‡] and Klaus Opwis*[,†]

[†]Deutsches Textilforschungszentrum Nord-West gGmbH, Adlerstrasse 1, D-47798 Krefeld, Germany

[‡]University Duisburg-Essen, Institute of Physical Chemistry and Center for Nanointegration, Duisburg-Essen, Universitätsstraße 5, D-45117 Essen, Germany

Supporting Information

ABSTRACT: Despite their excellent flame retardant properties, polyphosphazenes are currently not used as flame retardant agents for textile finishing, because a permanent fixation on the substrate surface has failed so far. Here, we present the successful synthesis and characterization of a noncombustible and foam-forming polyphosphazene derivative, that can be immobilized durably on cotton and different cotton/polyester blended fabrics using photoinduced grafting reactions. The flame retardant properties are improved, a higher limiting oxygen index is found, and the modified textiles pass several standardized flammability tests. As flame retardant mechanism a synergistic effect between the immobilized polyphosphazene and the textile substrate was observed. The polyphosphazene finishing induces an earlier decomposition of the material with a reduced mass loss in thermogravimetric analysis. The decomposition of cotton and polyester leads to the formation of phosphorus oxynitride, which forms a protecting barrier layer on the fiber surface. In addition, the permanence of the flame retardant finishing was proven by laundry and abrasion tests.

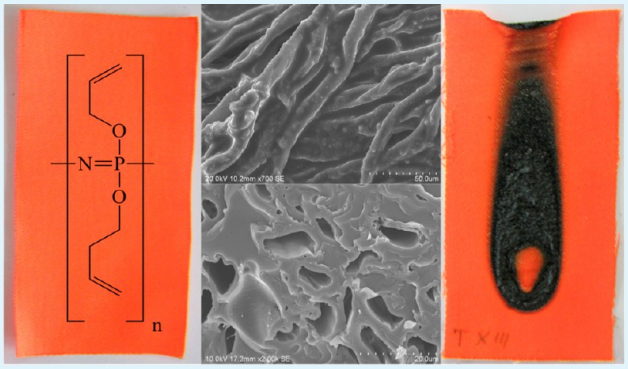

KEYWORDS: *cotton, polyester/cotton blends, textiles, polyphosphazenes, permanent flame retardant finishing, photochemical immobilization*

1. INTRODUCTION

Textiles made of natural and synthetic polymers such as cotton (CO), polyester (PET), or polyamide (PA) are omnipresent in our day-to-day life. Besides apparel, typical indoor applications are curtains, carpets, bedding, or upholstered furniture. Because of their high flammability, these materials represent a potential hazard for goods and life.[1] To achieve flame retardant textiles, the polymers are usually blended or finished with inorganic salts (e.g., nontoxic aluminum or magnesium hydroxide), organohalogens (e.g., chloroparaffins, bromobiphenylether, and bromobisphenols), or formaldehyde-based flame retardants.[1−4] Because of their high toxicity, the political pressure is growing steadily to replace halogen- and formaldehyde-based flame retardants.[5−10] Due to the fact that conventional organo-halogen-based flame retardants are getting banned more and more,[9] several halogen-free substitutes have been developed, e.g., polyphosphates, organic phosphates, or nitrogen compounds.[11] In this context nitrogen- and phosphorus-containing chemicals are especially interesting, because of their P−N synergistic effect[12] in flame retardant applications. However, their low stability with regard to washing and mechanical abrasion[13,14] is limiting their applicability. Furthermore, an increasing amount of organo-phosphorus derivates from flame retardants are found in the environment[15−17] and even in human tissue.[18] Some of these substances have a potential hormone-like effect.[19] Thus, alternative products that combine safety, high flame retardant properties, and the possibility to fix them permanently to the textile matrix are still desirable. One new approach to achieve flame retardant textiles is the use of layer-by-layer coatings, e.g., the combination of cationic polyelectrolytes such as polyallylamine,[20−22] chitosan,[23,24] or polyethylenimine[25,26] with anionic nanoclays,[20,24,26−28] polyphosphates,[20,23,25,29] or DNA.[30] Other strategies are based on sol−gel chemistry,[31,32] carbon nanotubes,[29,33,34] poly(carboxylic acid),[35−38] casein coating,[39] and photo-[40−42] or plasma-grafting.[27,43,44] More information on textile flame retardants is given in different reviews[45,46] and books.[2,10,11,13]

Another group of promising flame retardant materials are polyphosphazenes (PPZ), which can be divided into three different polymer types: linear polyphosphazenes and polymers with cylcophosphazene units (backbone or side chain).[47] These materials exhibit high limiting oxygen indices[48,49] and improve the flame retardant properties of polymer blends significantly.[49] Technically, polyphosphazenes are used, e.g., in hydrocarbon

Received: August 4, 2014
Accepted: April 22, 2015
Published: April 22, 2015

DOI: 10.1021/acsami.5b02141
ACS Appl. Mater. Interfaces 2015, 7, 9349−9363

insoluble O-rings,[50] in biomedical applications,[51] as bioinert[52] or biocompatible[52] coatings, or in fuel cell membranes.[47,50] A small number of textile finishings based on polyphosphazenes are already described. Shukla and Arya[53] showed that poly(fluorophosphazene) in combination with organo-bromine compounds improves the flame retardant properties of PET, while it is still unclear if the effect depends on the bromine-containing compounds or the polyphosphazene. Other textile applications for polyphosphazenes as finishing agents,[54] in textile polymer blending,[55] or in a polyurea coating are described in patents. Even fully inorganic polyphosphazenes such as (poly)aminophosphazene,[56,57] phospham,[58] phosphorus oxynitride,[59] and cylcophosphazenes[49,60−62] have been used as flame retardants. While these examples demonstrate the general usefulness of polyphosphazenes as flame retardants, no commercial textile PPZ-based finishing is available. The main reasons for this are the lack of polyphosphazenes with appropriate anchor groups for the durable fixation on the fiber surface and suitable process technologies. Because of our experience in the field of photoinitiated reactions for the surface functionalization of textile substrates,[40,63−65] our goal was to develop a flame retardant linear polyphosphazene with sufficient side-chain functionalities, that allow photochemical covalent bonding to typical textile materials, e.g., cotton and cotton/polyester blends.

Generally, polyphosphazenes can be synthesized by different synthetic routes.[66] The most common route is the high temperature ring opening polymerization of the cyclic trimer hexachlorophosphazene in a sealed glass tube developed by Allcock et al.[66] A solvent-based synthesis was developed by the group of Magill[67] that produces polymers with up to 15,000 monomer units (Scheme 1). The substitution of the chlorine

Scheme 1. Synthesis of Allyl-oxy-polyphosphazene

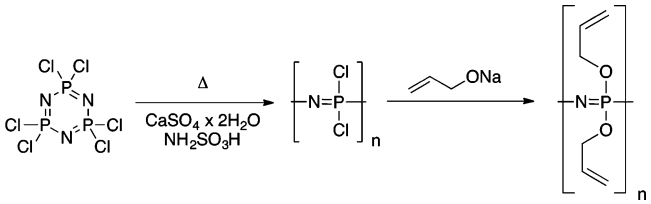

atoms by, e.g., alkoxy, phenoxy, amino, or fluoroalkoxy groups or even mixtures of them results in chemically and thermally stable species.[48,66] Due to the huge variety of possible side-chain functionalities, the properties of polyphosphazene derivatives can be varied easily, e.g. from water-soluble to highly hydrophobic polymers.[50]

This work is divided into three parts. First, the synthesis and the photochemical immobilization of an allyl-functionalized PPZ derivative are described. The second part includes the characterization of the thermal stability and the flame retardant properties of the PPZ-finished textiles by means of typical standardized combustion tests. Third, a possible flame retardant mechanism is discussed.

2. EXPERIMENTAL SECTION

2.1. Textiles and chemicals. The experiments were carried out using a commercial cotton woven fabric (twill 3/1, 230 g/m^2, white, CHT R. Beitlich GmbH, Germany), a commercial 50/50 CO/PET woven fabric (warp satin 4/1, 340 g/m^2, orange, Huntsman Textile Effects GmbH, Germany), and a commercial 50/50 CO/PET core yarn fabric (twill 2/1, core PET, CO shell, 170 g/m^2, camouflage, Bluecher GmbH, Germany). Hexachlorotriphosphazene was obtained from Eurolabs Limited (United Kingdom) and allyl alcohol (≥99%) from Merck (Germany). Sulfamic acid (≥99.3%), calcium sulfate ($CaSO_4 \times 2H_2O$, ≥98%), and tetrahydrofuran (THF, ≥99.9%) were obtained from Carl Roth (Germany). 1,2,4-Trichlorobenzene (≥99%), sodium hydride (55−65%, moistened with oil), and acetylacetone (≥99%) were obtained from Sigma-Aldrich (USA).

2.2. Instrumentation. Fourier transform infrared spectroscopy (FT-IR) was carried out using an IR Prestige by Shimadzu (Europe); for the attenuated total reflection (ATR) mode, a Silver Gate, Ge crystal, Specac (UK) with a resolution of 4 cm^{-1} was used. Differential scanning calorimetry was measured using a DSC Q20 (TA Instruments, USA) under 50 mL/min N_2 and a heating rate of 10 K/min. Thermogravimetric analyses (TGA) were measured with a TG 209-TASC 414/3 Thermal Analysis Controller (Netzsch, Germany). ^{1}H, ^{13}C, and ^{31}P nuclear magnetic resonance spectroscopy (NMR) was conducted using a Bruker DMX300 (USA) and a deuterated solvent as internal standard. Scanning electron microscopy (SEM) was done using a SEM S-3400 N II, Hitachi High-Technologies Europe with an integrated energy disperse X-ray unit (EDX, X-Max 50 mm^2 SDD Detector, Oxford Instruments, UK). An Ultraviolet A (UVA) print system lamp (Type 100−200, HPV-E2, H emitter with dichroitic reflector for IR reduction, power 200 W/cm, Hoenle UV Technology, Germany) served as a broadband UV-source. Standardized washing tests were carried out using a linitester by Atlas Material Testing Technology (Germany). Abrasion tests were conducted using with a Nu-Martindale (James H. Heal & Co., UK). Inductively coupled plasma optical emission spectra (ICP/OES) were measured using a Varian 720-ES spectrometer (Varian, Germany). Microwave digestion was done using a MarsXpress instrument (CEM, Germany).

2.3. Synthesis and characterization of allyl-oxy-polyphosphazene (PPZ). Freshly sublimated hexachlorotriphosphazene (40 g), sulfamic acid (170 mg), and $CaSO_4 \cdot 2H_2O$ (150 mg) were dissolved in 32 mL of 1,2,4-trichlorobenzene under a nitrogen atmosphere and heated to 210 °C for 45−60 min. At the end of the reaction, a strong increase of the viscosity can be observed. The chloropolyphopshazene was precipitated by the addition of dry petroleum ether, and the solids were washed twice with petroleum ether. The obtained polymer was dissolved in 100 mL of THF. The concentration of the solution was determined by evaporating an aliquot and weighing of the residue. Afterward, a freshly prepared sodium allyl alcoholate solution (4 equiv of allyl alcohol with 1.25 equiv of NaH in 50 mL of THF) was added. The reaction mixture was rigorously stirred for 4 h at room temperature (RT) and then refluxed for 6 h. The PPZ was precipitated by the addition of water. ^{1}H NMR (300 MHz, THF-d_8): δ 5.93 (ddt, J = 17.2, 10.4, 5.1 Hz, 1H), 5.29 (dd, J = 17.2, 1.8 Hz, 1H), 5.05 (dd, J = 10.4, 1.7 Hz, 1H), 4.48 (d, J = 5.5 Hz, 2H). ^{13}C{^{1}H} NMR (75 MHz, THF-d_8) δ 135.8, 116.0, 30.7. ^{31}P NMR (122 MHz, THF-d_8): δ −7.71. IR (ATR): 802 (P−O−C), 864, 923, 991, 1024 (P−N-backbone), 1101 (P−O-R), 1232 (P═N-backbone), 1423 (P−O−C), 1458 and 1647 (C═C), 2854 (C−H, sp^3), 2924 (C−H, sp^3), 3016 (C−H, sp^2), 3076 (C−H, sp^2) cm^{-1}. DSC (10 K/min, N_2 (50 mL/min)): T_G 180 °C, T_{Decomp} 282 °C.

2.4. Fabric UV treatment and characterization of the fixed PPZ. PPZ was dissolved in acetylacetone (25 wt %). The fabrics were wetted with 1 mL/g textile of the PPZ solution. The fabrics were irradiated single-sided for 10 min under an argon atmosphere. The distance between the light source and the sample was 20 cm. Subsequently, each sample was washed once in a textile linitester to remove nonbonded PPZ, afterward dried at RT and weighed. In order to determine the phosphor content of the textiles quantitatively, 0.4 g were digested with 8.0 mL HNO_3 (65%) in a microwave digester at 180 °C. After digestion, the samples were diluted to 25 mL with water and measured by ICP-OES. The error of the phosphorus determination is less than 5%. The add-on (A [wt %]) was calculated using eq 1, with W_0 = before irradiation, W_1 = after irradiation and washing.

$$A = \frac{W_1 - W_0}{W_0} \times 100\% \quad (1)$$

DOI: 10.1021/acsami.5b02141
ACS Appl. Mater. Interfaces 2015, 7, 9349−9363

2.5. Measuring of the thermostability. TGA was carried out under nitrogen (50 mL/min) with a heating rate of 10 K/min in an aluminum oxide crucible with precisely weighted sample sizes between 7 and 20 mg. The thermal oxidative decomposition was done under air in a preheated muffle furnace. After reaching the desired temperature, the PPZ-modified fabrics were kept inside for 10 min. Pure PPZ samples were prepared by dripping a PPZ solution on a KBr disc followed by UV irradiation.

2.6. Analysis of the thermal oxidative decomposition by IR. Samples of 5 cm × 5 cm PPZ-finished textiles were put into a preheated muffle oven at 200, 240, 280, 380, and 500 °C for 10 min under air. Afterward ATR-IR spectra of the fabrics were measured.

2.7. Washing resistance and abrasion test. In order to evaluate the washing fastness of the modified textiles, the materials were washed up to six times in a linitester according to EN ISO 105-C06 (liquor volume 150 mL, liquor ratio 1:80, ECE detergent 4.0 g/L, 30 min, 40 °C). The samples were then dried at room temperature and weighed. To investigate the fastness against mechanical stress, the modified textiles were subjected to 5,000, 10,000 or 50,000 abrasion cycles with a pressure of 9 kPa in a Martindale apparatus (abrasion test). Afterward the samples were weighted. For the test an inverted Martindale setup has been used to get samples of at least 5 cm × 10 cm for a flammability test. The sample size was 140 mm diameter and the abrasive cloth (Martindale SM 25 (ISO 12947-1)) 40 mm diameter, with an abrasive exposed area of 110 mm diameter.

2.8. Evaluation of the flame retarding properties. All flame retardant and LOI measurements were carried out after at least one washing cycle. The flame retardant properties were measured according to DIN EN ISO 15025 (protective clothing - protection against heat and flame - method of test for limited flame spread), with a reduced sample size of 5 cm × 10 cm and a Proxxon lighter (combustion gas butane). In addition, selected samples were tested externally by Staatliches Pruefamt fuer das Textilgewerbe - University of Applied Science Hof (Germany). One sample set was tested according to DIN EN ISO 15025, two sets according to DIN 75200 respectively US FMVSS 302 or ISO 3795 (motor vehicle safety standard), five sets according to EN ISO 11925-2 German, "Kleinbrenner" methode and five sets according to DIN EN ISO 4589-2 (limiting oxygen index (LOI, 0.5 % steps)).

3. RESULTS AND DISCUSSION

3.1. Synthesis of allyl-oxy-polyphosphazene (PPZ). PPZ was successfully synthesized by ring-opening polymerization of cyclic hexachlorotriphosphazene and subsequent nucleophilic substitution of the chlorine atoms by allyl alcoholate as shown in Scheme 1. The material is well soluble in acetylacetone. The ^{31}P NMR spectrum exhibits one singulett at −7.61 ppm, which indicates the presence of a non-cross-linked polymer with a typical chemical shift for a polyphosphazene. In addition, the ^{1}H NMR spectrum exhibits the typical signals for an allyl group (NMR spectra are shown in the SI). This correlates with the IR bands at 1232 cm^{-1} (P═N band) and at 1024 cm^{-1} (P−N band), which are characteristic bands for the polymeric backbone. The band at 1101 cm^{-1} represents the signal for the P−O−C ether. To achieve flame retardant properties, the flame retardant should have a decomposition temperature lower than the textile. Using DSC, we found a sharp exothermic degradation peak at 282 °C. When heating PPZ up to 600 °C, the polymeric material shows an intumescent behavior. The foam-formation is shown in Figure 1. In the case of fire, the foam layer can act as a heat barrier. A similar synthesis was developed and patented by Imada, where the polyphosphazene was used for blending PET.[68]

3.2. Textiles used in this study. For our studies, we chose three different kinds of fabrics, one cotton fabric and two CO/PET blends (both 50/50 mixtures) used in common textile applications (e.g., clothing including protective clothing, car interior, and furniture), where an improvement of the flame retardant properties is highly desired. The CO/PET blends differ in their fabric construction. The orange fabric is a warp satin woven material with one CO and one PET side. The second fabric (camouflage) consists of a PET core yarn with CO in the shell.

Figure 1. PPZ after heating in an oven to 600 °C.

3.3. Photochemical bonding of PPZ to textile materials. Besides phosphorus and nitrogen, which are responsible for the flame retardant properties of polyphosphazenes, our PPZ contains allyl groups, which are suitable for photoinduced grafting and cross-linking/homopolymerization. After wetting the textiles with a PPZ solution, the materials were irradiated by a broadband-UV lamp under an argon atmosphere. Before characterization, the materials were washed once to remove nonbonded compounds. The PPZ-modified textiles were characterized by gravimetric measurements, ATR-FT-IR and SEM in combination with EDX for surface morphology and composition. Total phosphorus content was measured by ICP-OES after digestion. Table 1 summarizes the results. After the first washing step a high add-on of PPZ between 20 and 40 wt % was determined by gravimetry. An average weight loss after one washing step in the range of only 2−3% proves the general efficiency of our photoinduced immobilization method. The phosphorus content found by ICP-OES is close to the calculated P content obtained by gravimetry. The surface P determined by EDX is between 18.5 and 22.5 wt %, which correlates with the mass fraction of P in the PPZ. Therefore, the layer thickness of immobilized PPZ

Table 1. Summary of Calculated and Measured Values for the P Content of Two Cotton/Polyester Blends and a Cotton Fabric

Textile	Add-on [wt %]	P calculated from add-on [wt %]	P measured[a] [wt %]	P surface[b] [wt %]	P mass fraction[c] [wt %]
CO (white)	40.8	5.7	4.9	18.8	19.5
CO/PET (orange)	22.3	3.6	3.1	18.5	
CO/PET (camouflage)	32.8	4.8	4.2	22.7	

[a]Measured quantitatively by ICP-OES. [b]Measured qualitatively by EDX. [c]Calculated from $[C_6H_{10}NPO_2]_n$ (see Scheme 1).

DOI: 10.1021/acsami.5b02141
ACS Appl. Mater. Interfaces 2015, 7, 9349−9363

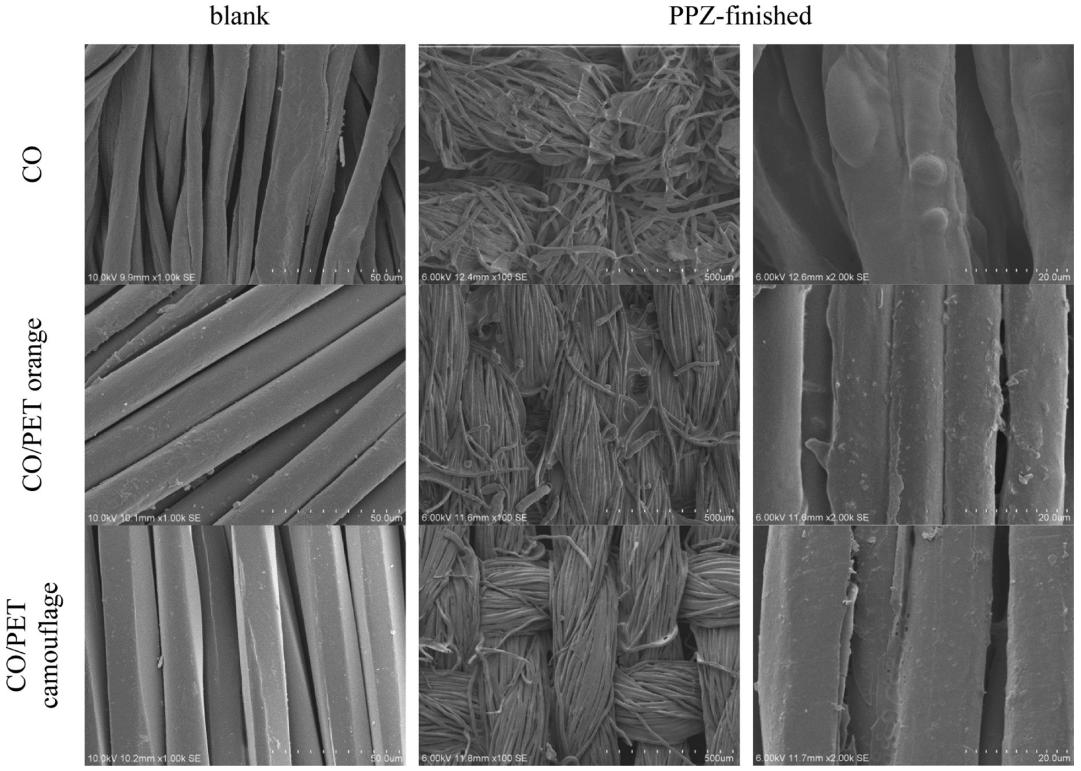

Figure 2. SEM micrographs of cotton fabrics and cotton/polyester blends before and after PPZ finishing (after one laundering cycle).

must be higher than the information depth of the used EDX technology—thus at least 1.0 μm. The measured phosphorus contents (about 4 wt %) are higher than the recommended value for flame retardant properties[1] (>1.5 wt %). Accordingly, flame retardant properties for the PPZ finished textiles can be expected. SEM micrographs (Figure 2) show a film deposition of PPZ on the textiles surface. As a consequence, the corresponding ATR-FT-IR spectra of the textiles (Figure 3)

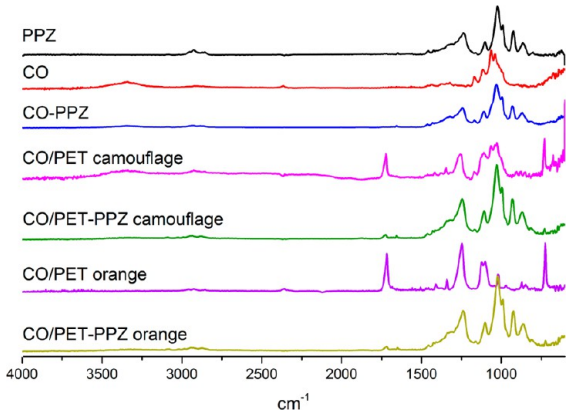

Figure 3. ATR-IR-spectra of cotton/polyester blends and cotton fabrics before and after PPZ finishing in comparison to pure PPZ (black line).

change completely to the IR signals of pure PPZ; only the strong substrate signals such as the carbonyl band of the PET part of the blends or the OH-signal of CO are weakly left. Taking the high add-on and the corresponding thickness of the PPZ layer into account, we assume that the PPZ is mainly bound by photoinduced homopolymerization between PPZ polymer chains yielding a stable film surrounding the fiber.

3.4. Thermal stability. TGA measurements in nitrogen provide information regarding the thermal stability of a certain material (see Table 2). Various studies have demonstrated that good flame retardant properties of a finishing correspond with a decrease of the decomposition temperature and an increase of the remaining residue (Res) compared to the unfinished textile. In Figure 4, the (D)TG thermograms of finished and unfinished fabrics are shown. Below 100 °C, adsorbed water evaporates and a first weight loss of 1−3% can be observed. The untreated cotton sample shows one single thermal decomposition step at 360 °C, which is related to the depolymerization by trans-glycosylation reactions[32] of cotton. As observed by Carosio et al.,[23] a two step decomposition for both untreated CO/PET blends was found. The first represents the depolymerization of CO, and the second derives from the PET depolymerization. In the case of the PPZ-finished textiles, an extra decomposition step was found. Moreover, in all investigated cases the decomposition ($T_{-5\%}$) starts earlier compared to the untreated materials. The first observed decomposition step starts at 240 °C and is accompanied by a low weight loss of about 5% at T_{max}. The second step at nearly 280 °C yields a higher weight loss and a fast reaction. This second step correlates with the PPZ decomposition temperature measured by DSC. Next, the phosphoric acid formed induces the char formation of the cotton portion.[32,69] The last step represents the earlier and slower decomposition of PET by phosphoric acid cleavage of the ester bonds. For all PPZ-finished samples, a significantly higher residue remains due to the catalyzed char formation. In addition, the PET part of the blended material decomposes at lower temperatures. This kind of shift for PET in blends has not been reported before.

3.5. Flame retardant properties. In order to evaluate the flame retardant properties of the textiles, various methods were used. By measuring the limiting oxygen index (LOI), the

DOI: 10.1021/acsami.5b02141
ACS Appl. Mater. Interfaces 2015, 7, 9349−9363

Table 2. Overview of the TGA Parameters of the Samples[a]

Sample	Res_{H2O} [%]	$T_{-5\%}$ [°C]	T_{max1} (Res) [°C (%)]	T_{max2} (Res) [°C (%)]	T_{max3} (Res) [°C (%)]	$Res_{700°C}$ [%]
CO	0.9	317	361 (46.0)	-	-	13.1
CO-PPZ	1.3	243	243 (90.5)	288 (72.1)	-	39.1
CO/PET ora.	1.8	328	348 (75.3)	428 (38.9)	-	19.1
CO/PET−PPZ ora.	0.8	246	238 (94.1)	276 (87.0)	375 (54.1)	31.7
CO/PET cam.	0.3	309	333 (79.6)	438 (33.7)	-	15.6
CO/PET−PPZ cam.	2.7	276	233 (91,8)	284 (81.2)	388 (52.1)	30.7

[a] T_{max} is obtained by the derived DTG curve.

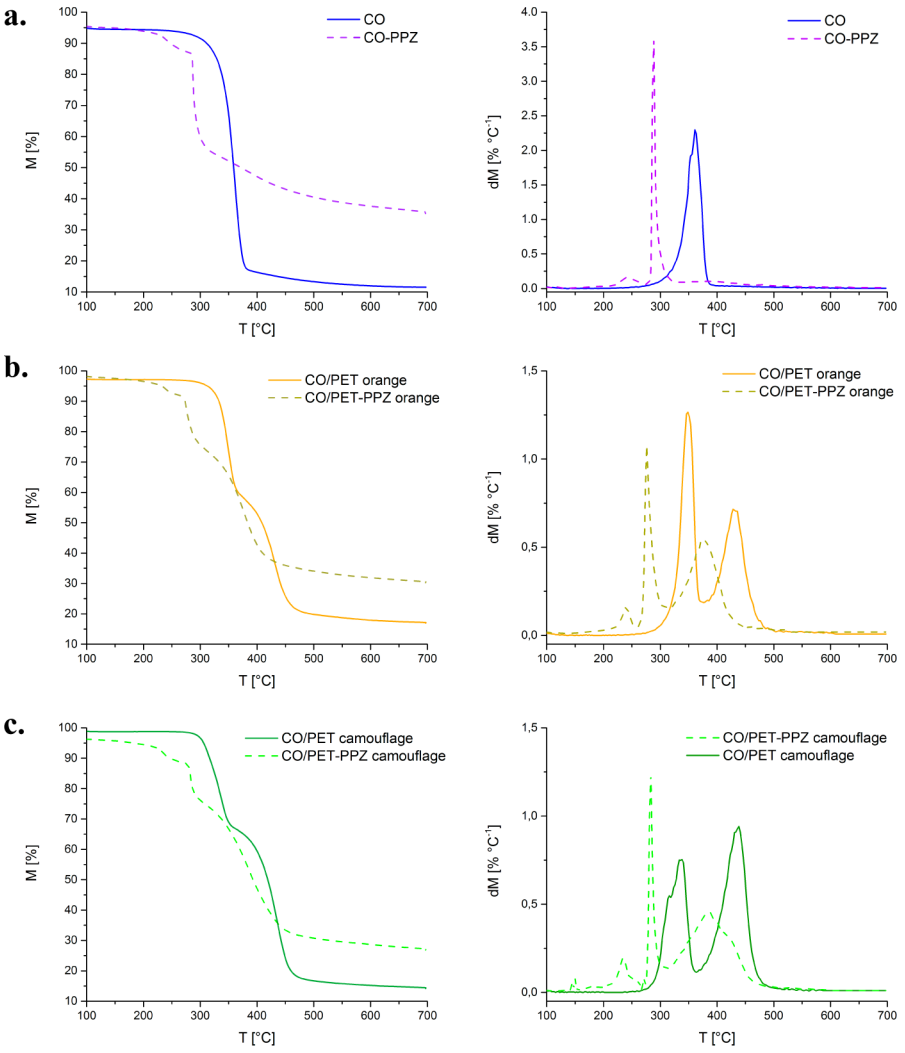

Figure 4. TG and DTG of PPZ finished and untreated textiles: (a) cotton; (b) CO/PET orange; (c) CO/PET camouflage.

Table 3. Comparison of the Test Conditions and the Passing Requirements

	DIN 75200	DIN EN ISO 15025 A1	EN ISO 11925-1
Flame gas	propane	propane	propane
Flame size	38 mm	25 mm	20 mm
Flame contact time	15 s	10 s	15 s
Ignition area	edge	face	edge
Sample size	100 mm × 356 mm	150 mm × 200 mm	90 mm × 190 mm
Sample alignment	horizontal	vertical	vertical
Passed:	Burn rate: <102 mm/min	for DIN EN ISO 11611: no afterburning (after burn time ≤2 s after glow time ≤2 s no dripping no hole formation	for DIN 4102-1 B2 or EN ISO 13501-1 E: Flame tip does not reach measuring mark at 150 mm within 20 s

DOI: 10.1021/acsami.5b02141
ACS Appl. Mater. Interfaces 2015, 7, 9349−9363

Figure 5. Untreated and PPZ-finished textiles before and after in-house flammability test. *Sample holder is visible at the right and left edge of the picture and in the background.

minimum amount of oxygen in a mixture of oxygen and nitrogen is determined that is required to keep an ignited polymer burning. Normally, an increased LOI is accompanied by a lower ignitability and, therefore, improved flame retardant properties. For different textile applications, different flammability testing standards exist. Here, we choose three methods. In the first test, the burning speed of a horizontal sample is measured; this test is described in DIN 75200 and is essential for textiles used in car interiors. DIN EN ISO 15025 represents a test for protective clothing. This test is relevant for protective clothing for fire fighters (DIN EN 469) or welders (DIN EN ISO 11611) and clothing for protection against heat and flame (DIN EN ISO 11612, DIN EN ISO 14116). The results of this test were classified according to DIN EN ISO 11611 (Protective clothing for use in welding and allied processes). In addition, the test EN ISO 11925-2 was carried out to achieve the classification "normal flammability" according to DIN 4102-1 class B2 or EN ISO 13501-1 class E for building materials. Because of the vertical edge ignition applied in this test, the conditions are highly ambitious for textiles. The testing conditions of the used methods are summarized in Table 3.

Figure 5 shows pictures of the PPZ-treated textiles after our in-house flammability test according to DIN 15052 compared to the untreated materials. While the untreated samples burn down completely, all PPZ-finished textiles exhibit a significantly improved flame retardant behavior. Though the flame reaches the upper edge of the samples (due to the reduced sample size of 10 cm × 5 cm instead of 15 × 20 cm), no hole formation was observed. In addition, the magnification of the burned samples (Figure 5, right column) illustrates a significant foam formation caused by the PPZ finishing. The formed foam is brittle and flakes off.

Table 4 summarizes the results of the various burning tests and the corresponding LOI measurements. Compared to the untreated materials, the LOI of the PPZ-finished textiles increases by 5−8%, which provides a first indication for a reduced flammability. During the horizontal burning test (DIN 75200), the untreated fabrics burn completely down with burn rates of 60−120 mm/min. In contrast, both modified CO/PET blends are self-extinguishing after the removal of the flame. In the case of modified CO, an acceleration of the burning was observed; however, the char yield is raised due to a significant carbonization of the material. By changing to a vertical flame test (DIN EN 15025), with a 10 s flame contact at the surface, the untreated materials burn down again completely. In contrast, the PPZ-modified cotton and the CO/PET orange

DOI: 10.1021/acsami.5b02141
ACS Appl. Mater. Interfaces 2015, 7, 9349−9363

Table 4. Results of the LOI Measurements and the Standardized Burning Tests on PPZ-Modified Textiles

	CO white	CO/PET orange	CO/PET camouflage
		LOI	
untreated	17.5−18.0	18.5−19.0	16.5−17.0
PPZ	23.0−23.5	26.5−27.0	24.0−24.5
		DIN 75200	
burning rate [mm/min]	142	0	0
comment	carbonization	-	-
test passed	**no**	**yes**	**yes**
burning behavior of untreated material	burns down completely, burning rate 98 mm/min	burns down completely, burning rate 59 mm/min	burns down completely, burning rate 119 mm/min
		DIN EN ISO 15025 for DIN EN ISO 11612	
Flame reaches upper or lateral edge	no	no	yes
afterflame time [s]	0	0	20
afterglow beyond flame area	no	no	no
afterglow [s]	0	0	0
appearance of particles	no	no	no
burning particles	no	no	no
hole formation	yes	no	no
comment	-	-	extinguishes almost, burns slow, carbonization
test passed	**yes**	**yes**	**no**
burning behavior of untreated material	burns down completely within 8 s	burns down completely within 22 s	burns down completely within 11 s
		EN ISO 11925-2 for DIN 4102-1 B2	
reaching the test mark	7 s	5 s	4 s
max. flame height	>25 cm	>25 cm	>25 cm
moment of max. flame height	12 s	12 s	10 s
self-extinguished	0 s (during flame impingement)	0 s	5 s
dripping	no	no	no
test passed	**no**	**no**	**no**
burning behavior of untreated material	burns down completely 5 s reaches test mark	burns down completely 6 s reaches test mark	burns down completely 4 s reaches test mark

Figure 6. Blind and PPZ-finished textiles after the 15 s vertical flame test (EN ISO 11925-2). The test mark of 150 mm is visible as the blue line on the fabric.

blend do not keep burning after the removal of the flame and no afterglowing was observed. These results are in good correlation with our in-house test. However, the results for the other CO/PET blend (camouflage) do not fully correlate with the modified test (see Figure 5). In this case, the material starts to burn and only a carbonized residue was obtained, probably the add-on was too low or uneven. Finally, the three textile materials were subjected to a fire test with a 15 s vertical edge flame impingement test. All PPZ-modified textiles do not pass the test requirements, because the flame reaches the upper test mark during impingement. However, a significant flame retardant behavior was observed. In contrast to the untreated materials, all PPZ-modified samples are self-extinguishing after the removal of the flame. Figure 6 illustrates the strong improvement of the flame retardant properties of PPZ-finished textiles compared to the blank substrates.

3.6. Characterization of the formed char. A compact char layer acts as a barrier and can help to protect the fiber against heat and flames. The morphology and composition of the formed char affects the flame retardant mechanism. Therefore, we characterized the char formed during the flame retardant test DIN 15025 with SEM, EDX, and ATR-IR. Figure 7 shows SEM micrographs of the PPZ-modified cotton after the burning test. The fabric structure of CO is preserved and the surface is covered with a bubble-like structure. The cross-section micrographs demonstrate the formation of hollow

DOI: 10.1021/acsami.5b02141
ACS Appl. Mater. Interfaces 2015, 7, 9349−9363

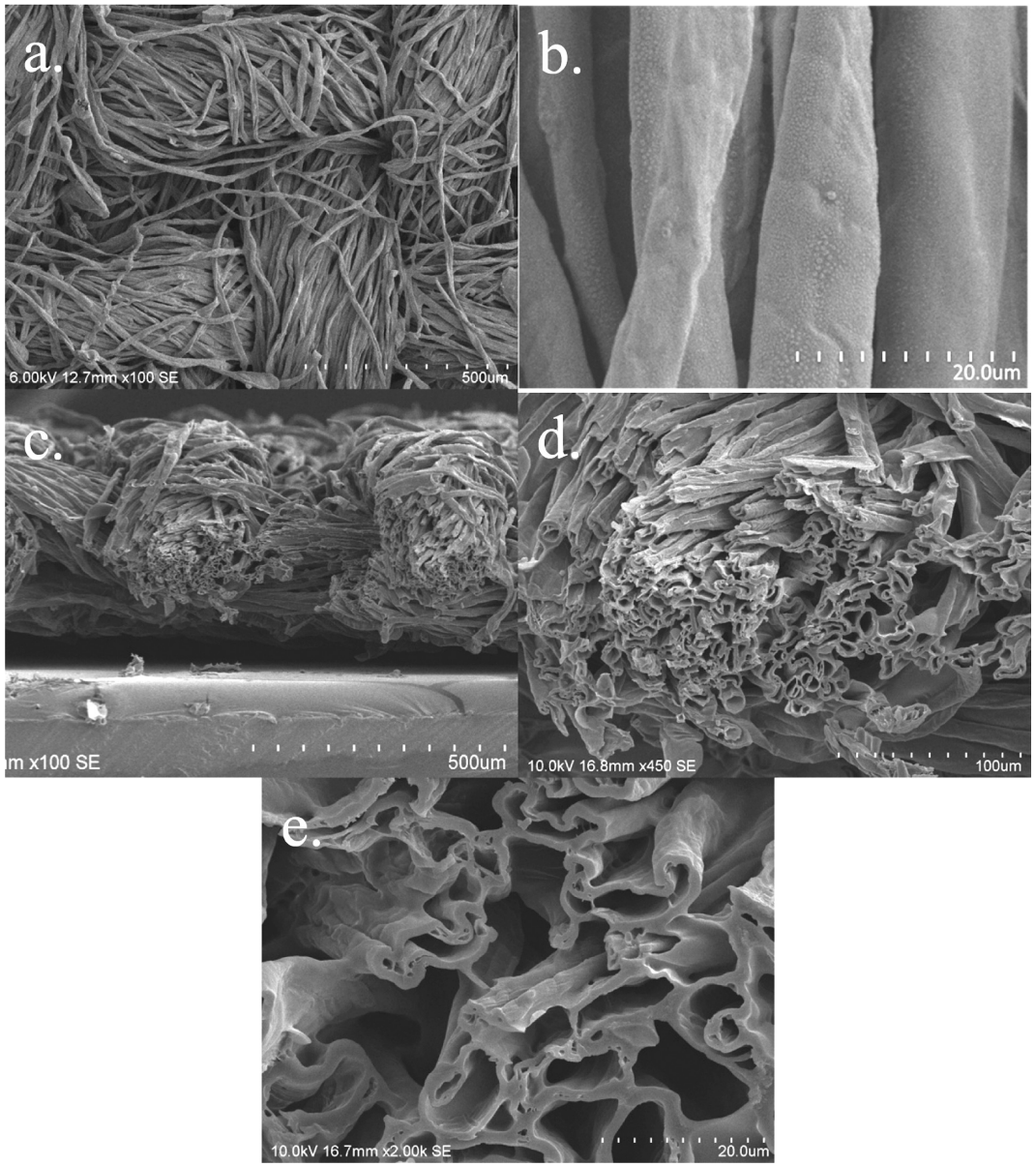

Figure 7. SEM pictures of charred PPZ-modified cotton fibers after the burning test according to DIN 15025: (a and b) top view of the charred fabric; (c–e) cross sections of the fibers.

fibers, thus hinting at the assumed stable film of homopolymerized PPZ surrounding the fiber, while the cotton core was decomposed and carbonized fully during combustion.

In all cases, the PPZ-modified textiles exhibit a brittle foam layer after the burning test. Underneath the peeled-off layers, fibers are visible. For further SEM investigations we defined two positions: P1, where the foam flakes off, and P2, the foam surface. Figures 8 and 9 show the corresponding SEM micrographs of the orange and respectively the camouflage PPZ-modified CO/PET fabric. In both cases, the fiber structure under the foam layer (P1) is still intact and the embedment of the fibers in the PPZ matrix is visible in the top view (Figures 8a-b and 9a-b) and also in the cross sections (Figures 8f and 9f). In addition, Figures 8b and 9b disclose a subtle bubble structure on the fiber surface (Figures 8b and 9b). The cross sections (Figures 8d and 9d) correspond to the visual observation that the foam layer is thicker on the orange fabric. The foam itself (P2) forms a close layer with some pinholes (Figures 8c and 9c). As for CO, the formation of hollow fibers can be observed (Figures 8e-f and 9e-f). Additional EDX measurements at P1 (fibers under spalled foam) and P2 (foam surface) revealed a 20% phosphorus content at both positions.

Char of PPZ-modified CO. The IR spectra of charred CO (Figure 10b) exhibit four broad signals at 1606, 1192, 940, and 840 cm^{-1}. 1606 cm^{-1} is clearly assignable to the C═C absorption, whereas the broadness of the signal at 1192 cm^{-1} alludes to multiple signals, e.g., the P═O stretching band (1150 cm^{-1}), the P–O–P (symmetrical stretching typical around 1090 cm^{-1}), and the P═N (1260–1220 cm^{-1}) absorption. 940 cm^{-1} can be assigned to P–O–P (asymmetrical stretching) and 840 cm^{-1} to P–O–C absorption. The formation of the C═C double as part of a graphite-like char is a result of the dehydration of CO. The broad signals, which are assignable to different P–O and P–N groups, are typical for phosphorus oxynitrides (PON)[59,70] bonded to the graphite-like char (P–O–C signal 840 cm^{-1}).

DOI: 10.1021/acsami.5b02141
ACS Appl. Mater. Interfaces 2015, 7, 9349–9363

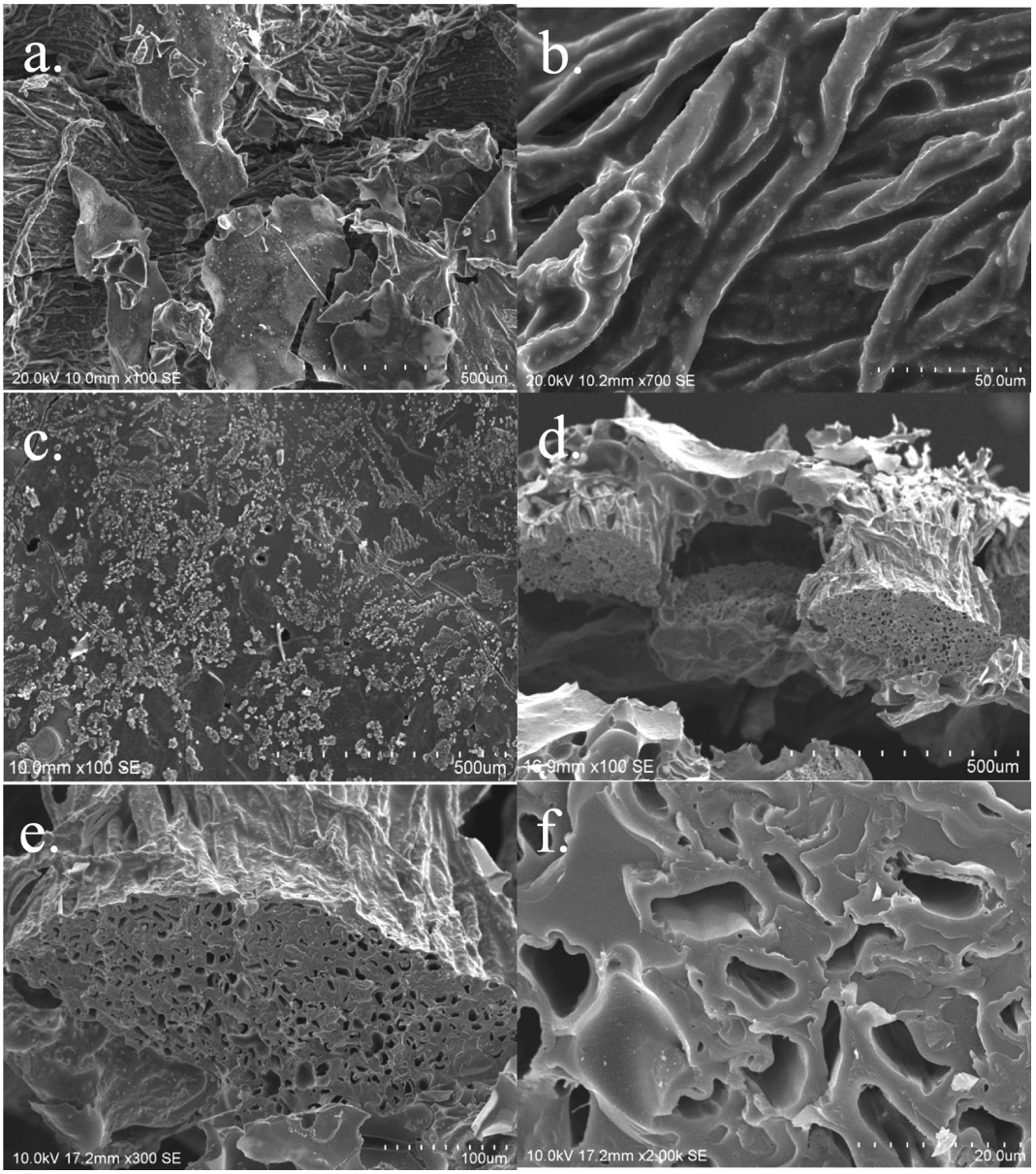

Figure 8. SEM pictures of charred PPZ-modified CO/PET fibers (orange) after the burning test according to DIN 15025: (a and b) top view on P1; (c) view on the foam layer P2; (d–f) cross sections of the fibers.

Char of the PPZ-modified CO/PET blends. Figure 10 shows IR spectra of P1 (Figure 10a) and P2 (Figure 10b) of PPZ-modified CO/PET blends after the burning test. At position 1 the spectra are very similar to the blank PET fabric (Figure 10a). Only slight differences relative to the reference can be observed: the charred samples contain no signals for C–H bonds, a shoulder next to the 1260 cm^{-1} band emerges, and the intensity ratio of the double peak at 1099 cm^{-1} changes in addition to the broadening of the signal.

The IR spectra of the foam layers (P2, Figure 10b) of both blended materials are comparable. Differences can be found in the carbonyl region, where the PPZ-modified orange CO/PET shows an additional band at 1690 cm^{-1} and a broad weak signal at 1443 cm^{-1}. Moreover, the 974 cm^{-1} band has a higher intensity than the PPZ-modified camouflage fabric. An unambiguous assignment is not possible, since PET has comparable signals, e.g. at 1720 cm^{-1} (carbonyl group), 1260 cm^{-1} (asymmetric stretching CO–O–C), and 1100 cm^{-1} (stretching C–O–C). The 1690 cm^{-1} can be assigned to α–β unsaturated carbonyl groups or typical C═C signals from aliphatic or aromatic carbons after thermal dehydration. The signals between 1261 and 1120 cm^{-1} correspond to P═N or P═O bonds or to PET itself. The signals at 1097 and 974 cm^{-1} belong to the symmetrical and asymmetrical stretching of P–O–P groups, and the band at 875 cm^{-1} can be assigned to P–O–C absorption. In summary, the IR spectra of the foam layer (P2) suggest a mixture of PET and PON and fit perfectly to the corresponding EDX data.

On the other hand, the IR spectra of P1 indicate a surface composition of pure PET, while EDX results in 20% phosphorus content. To clarify this obvious contradiction, we investigated the decomposition of the used materials at specific temperatures. The PPZ-finished fabrics were heated under air for 10 min up to 200, 240, 280, 380, and 500 °C. In addition, pure PPZ was heated up to 700 °C. Figure 11 shows the corresponding ATR-IR spectra of the residual material after

DOI: 10.1021/acsami.5b02141
ACS Appl. Mater. Interfaces 2015, 7, 9349–9363

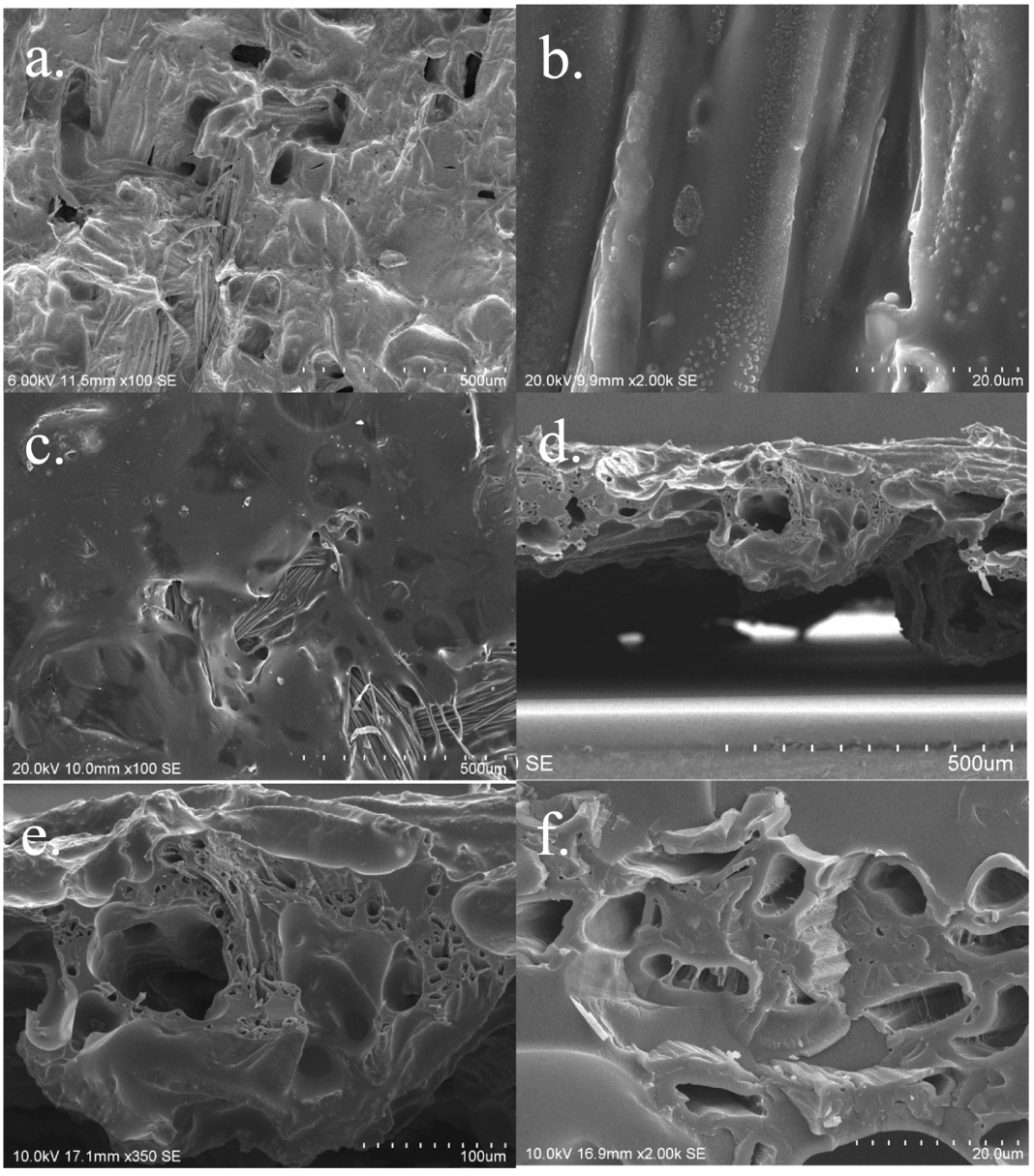

Figure 9. SEM pictures of charred PPZ-modified CO/PET fibers (camouflage) after the burning test according to DIN 15025: (a and b) top view on P1; (c) view of the foam layer P2; (d–f) cross sections of the fibers.

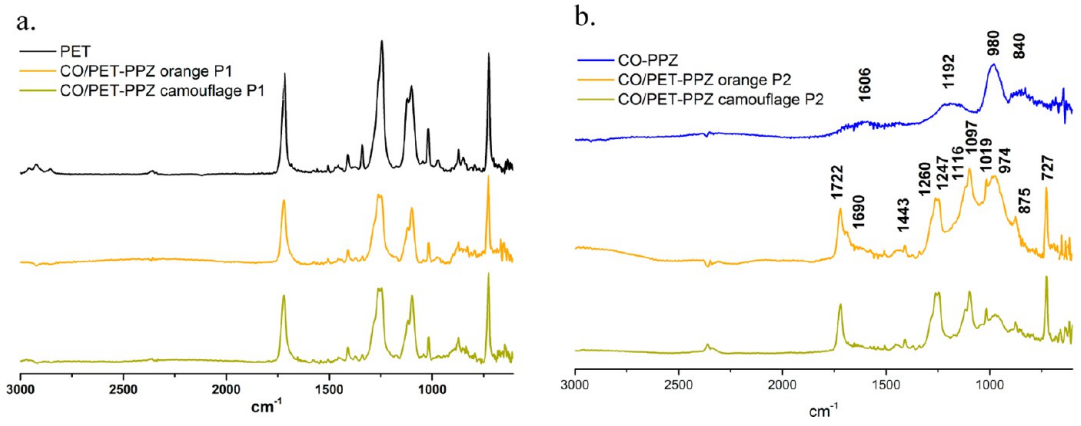

Figure 10. ATR-IR spectra of (a) the foam free part of the blend (P1) in comparison to PET and (b) the charred CO and foam layer of the blends (P2).

DOI: 10.1021/acsami.5b02141
ACS Appl. Mater. Interfaces 2015, 7, 9349–9363

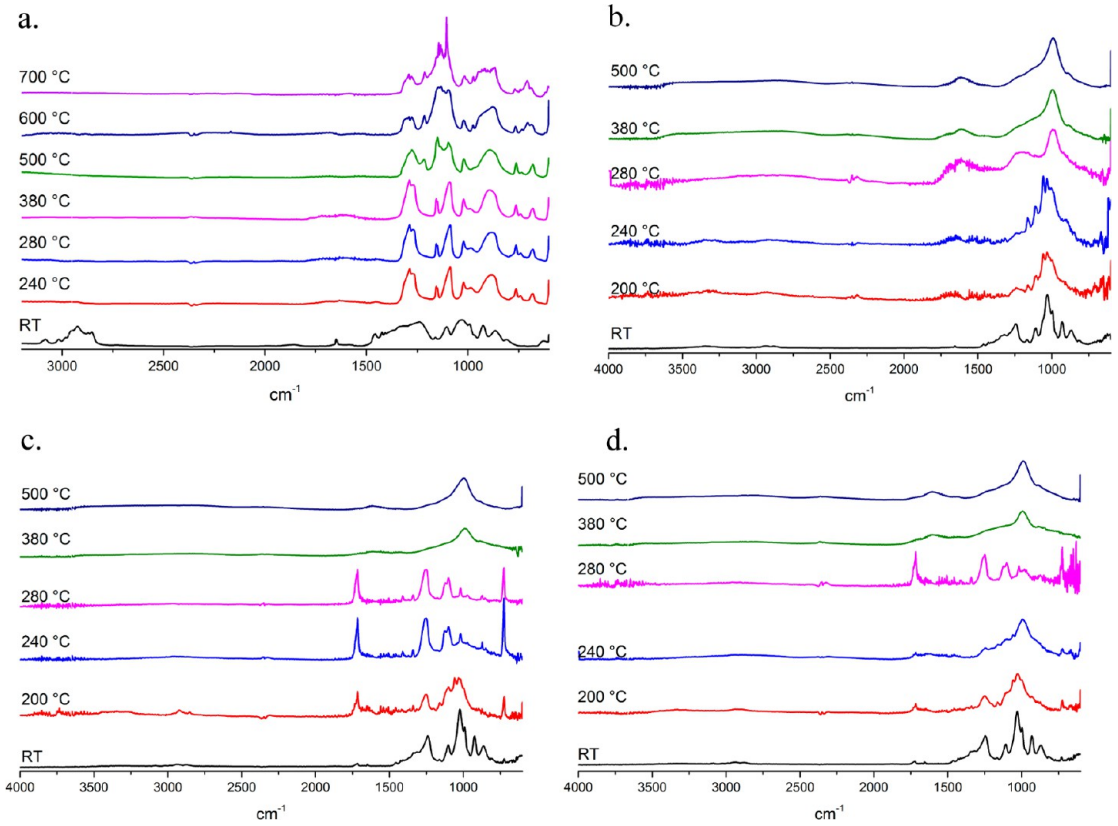

Figure 11. ATR-IR spectra of the thermal oxidative decomposition of (a) PPZ, (b) CO-PPZ, (c) CO/PET−PPZ orange, and (d) CO/PET−PPZ camouflage.

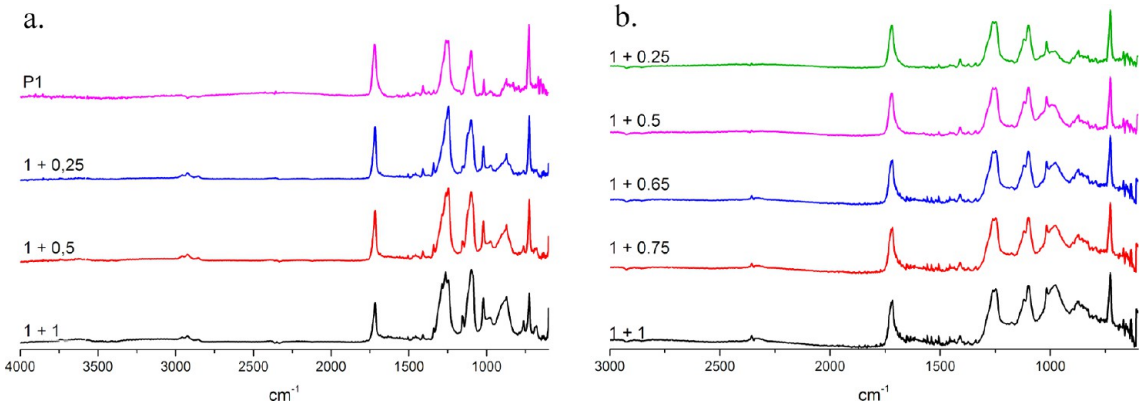

Figure 12. Simulation of the IR-spectra by addition of different ratios: (a) P1 by PET + PPZ 280 °C spectra; (b) P2 blend 280 °C + PON.

treatment (photographs are given in the Supporting Information). During heating, the IR spectra of pure PPZ change significantly at 240, 500, and 700 °C (Figure 11a). The corresponding decomposition signals at 1250 and 1100 cm^{-1} are similar to PET. However, up to 700 °C no PON formation was observed.

As shown in Figure 11d the decomposition of the shell/core CO/PET (camouflage) material starts at 240 °C with the outer PPZ-cotton layer (similar to the pure PPZ-CO material in Figure 11b) followed by the decomposition of the inner PET core at 280 °C. At 380 °C, there is strong evidence for the generation of PON, because the characteristic signals at 1190 and 980 cm^{-1} are observed. In the case of the mixed CO/PET fabric (orange), IR signals for the decomposition of the cotton and PET parts arise simultaneously between 240 and 280 °C, which hints at the graphitization of the material and the formation of PON (Figure 11c). At 500 °C, the spectra of all fabrics are similar to each other.

For both the thermal oxidative decomposition of PPZ-modified cotton and the decomposition of it by combustion (burning tests), the formation of a graphite/PON char was observed. On the other hand, this was not found in the case of PPZ-modified CO/PET blended materials. The combusted materials (P1, Figure 10a) seem just to be exposed to a temperature of 280 °C (Figure 11c and d). For P2 (Figure 10b) no comparable spectra were found in the thermal oxidative decomposition (Figure 11c and d). The signals at 980 and 1200−1000 cm^{-1} and their broadness can be interpreted as overlapping signals. The EDX spectra of both P1 and P2 result in similar amounts of phosphorus. For P1 it can be explained as

DOI: 10.1021/acsami.5b02141
ACS Appl. Mater. Interfaces 2015, 7, 9349−9363

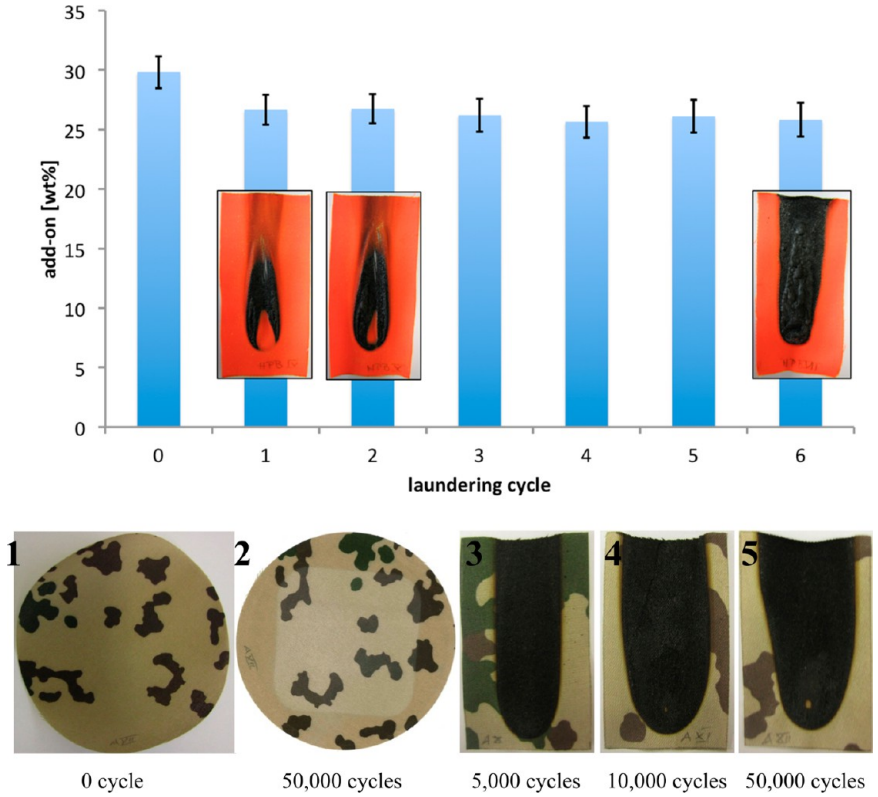

Figure 13. Top: Washing fastness. PPZ-add-on and flammability behavior after six washing cycles. Bottom: Abrasion fastness: (**1**) PPZ-modified textile before and (**2**) after Martindale test. (**3**–**5**) Samples after 5,000, 10,000, and 50,000 cycles in flammability test.

a combination of the IR of PET and the decomposed PPZ of 280 °C, and for P2 it is a combination of PON and the blend after 280 °C. To prove this theory, we simulated the IR spectra of P1 and P2 by summation of different ratios of the IR-spectra, that of P1 by PET and PPZ after 280 °C, and that for the P2 blend after 280 °C and PON. The IR-spectra of P1 can be calculated by summation in a ratio of 1 + 0.5 (PET + PPZ 280 °C, Figure 12a, different ratios are given). For P2 of CO/PET (orange) a 1 + 1 ration and for CO/PET (camouflage) a 1 + 0.5 ratio was found. On basis of the IR, mainly PET remains in the charred blends. This is verified by measuring the PET melting enthalpy by DSC, where we find a higher amount of PET in the charred samples. The DSC melting signal is broadened, which shows as partly PET decomposition.

Flame retardant mechanism. The TGA measurements of the CO/PET blends show an earlier thermal decomposition of PET, which has not been reported before. In addition, a higher amount of residue is observed. In combination with the intumescent behavior observed and supported by SEM imaging, it can be concluded that a protective layer is formed. Additional IR studies indicate that the layer contains PON after thermal oxidative treatment or 10 s flame contact. Based on the corresponding IR measurements, the decomposed PPZ-modified cotton consists fully of PON, while the PET/CO blends formed an outer PON/PET mixture. The PON layer works as a thermal isolator and protects the underlying material, even PPZ and PET. In contact with the flame, the PET melts underneath the PON layer and is pulled into the PON foam by capillary forces. As a result, the mixed IR spectra for P2 can be explained (Figure 10b). The thermal treatment of the pure PPZ indicates that even at 700 °C no PON is formed (Figure 11a); however, in combination with a fabric, the formation of PON starts already at 380 °C. This can be explained by a synergistic interaction between the decomposition of cotton and the PPZ. Cotton is dehydrated by the formed phosphoric acid. Afterward, the decomposition products of cotton support the formation of a protective PON layer.

3.7. Investigations on the permanence of the polyphosphazene finishing toward washing and abrasion. To evaluate the stability (fastness) of the PPZ modification, samples were subjected to several washing cycles and rigorous abrasive tests. Afterward, the flame retarding properties were investigated according to the modified DIN EN ISO 15025 conditions. Figure 13 (top) summarizes the add-on of the PPZ-layer on the orange CO/PET textile after different washing cycles. After the first washing cycle, noncovalently bonded PPZ was removed, which leads to a significant weight loss of nearly 3%. After the following washing cycles, no further weight loss was observed. Moreover, in all flame retardant tests, the specimens are self-extinguishing, accompanied by a formation of a carbonized layer (Figure 13, top). Although the flame reaches the upper edge after six laundering cycles, a strong permanence of the flame retardant effect against washing can be assigned.

In addition, the abrasion fastness of the PPZ-modified CO/PET (camouflage) blend was tested. After subjecting the textiles to 5,000, 10,000, or 50,000 abrasion cycles in a Martindale tester, the flame retardant properties of the materials did not change significantly. All samples are self-extinguishing after the removal of the flame.

DOI: 10.1021/acsami.5b02141
ACS Appl. Mater. Interfaces 2015, 7, 9349–9363

4. CONCLUSION

Polyphosphazenes belong to the class of inorganic polymers. Due to their phosphorus and nitrogen backbone, they exhibit excellent flame retardant properties. However, their industrial application in textile finishing was as yet limited by the lack of durable fixation strategies for a permanent flame retardant effect during the products lifetime. We succeeded in bonding a noncombustible and strongly foam-forming polyphosphazene derivative by an UV-induced grafting process to cotton and cotton/polyester blends in high add-ons up to 40 wt %. SEM imaging proves the successful immobilization, and a total phosphorus content between 3 and 5 wt % was found. The polyphosphazene finishing leads to textiles with higher LOI. The textiles exhibit improved flame retardant properties and pass several standardized flammability tests such as standards for protective clothing and automotive textiles. Char analysis indicates the formation of a phosphorus oxynitride layer during combustion, which is synergistically promoted by the textile material itself. The charred layer acts as a thermal isolating barrier layer and protects the underlying material. The permanence of the finishing was proven by washing and abrasion tests. The most essential results of PPZ-modified cotton and cotton/polyester blends are summarized in Table 5.

Table 5. Summary of the Flame Retardant Properties of PPZ-Modified Textiles[a]

test	CO white	CO/PET orange	CO/PET camouflage
LOI[b]	+	+	+
DIN EN ISO 15025 (protective clothes)[b]	+	+	(+)
DIN 75200 (automotive)[b]	−	+	+
DIN 4102-1 B2 (fire classification B2)[b]	(+)	(+)	(+)
washing fastness[c]	+	+	+
abrasion fastness[c]	+	+	+

[a]− = failed/no improvement, (+) = failed, but significant flame retardant effect, + = passed/strong improvement. [b]After one laundering cycle. [c]Modified DIN EN ISO 15025 procedure.

In consideration of these excellent results, we state that functional polyphosphazenes could be a new class of permanent and halogen-free flame retardant agents for textile applications in the near future. However, competitive and commercial products for the textile industry have to be water-based (water-soluble or at least water-dispersible). Therefore, a future focus will be the synthesis of innovative polyphosphazenes, which combine functional side groups for a permanent attachment and hydrophilic side groups for an improved solubility in aqueous systems.

■ ASSOCIATED CONTENT

Supporting Information

Photographs and IR and NMR spectra of blank and PPZ-finished textiles at different tempratures. The Supporting Information is available free of charge on the ACS Publications website at DOI: 10.1021/acsami.5b02141.

■ AUTHOR INFORMATION

Corresponding Author

*Phone: +49-2151-843-205. E-mail: opwis@dtnw.de.

Notes

The authors declare no competing financial interest.

■ ACKNOWLEDGMENTS

The authors wish to acknowledge financial support by the Forschungskuratorium Textil e.V. for the project IGF 16780 N. The support was granted within the program Industrielle Gemeinschaftsforschung (IGF) from resources of the Bundesministerium für Wirtschaft und Energie (BMWi) via a supplementary contribution by the Arbeitsgemeinschaft Industrieller Forschungsvereinigungen e.V. (AiF). We thank the Department of Analytics of the University Duisburg-Essen (Germany) for NMR spectroscopy, Hochschule Niederrhein - University of Applied Science (Krefeld, Germany) for TGA measurements, Staatliches Pruefamt fuer das Textilgewerbe - Hof University of Applied Science (Muenchberg, Germany) for measuring TGA, LOI, and standardized flammability tests, and DTNW Oeffentliche Pruefstelle GmbH for the ICP measurements.

■ REFERENCES

(1) Horrocks, A. R.; Price, D. *Fire Retardant Materials*; Woodhead Publishing Limited: Cambridge, UK, 2001.
(2) Horrocks, A. R.; Kandola, B. K. In *Plastics Flammability Handbook: Principles, Regulations, Testing, and Approval*; Troitzsch, J., Ed.; Hanser: Munich, Germany, 2004; pp 173−188.
(3) Guckert, D. J.; Lovasic, S. L.; Parry, R. F. In *Handbook of Building Materials for Fire Protection*; Harper, C. A., Ed.; McGraw-Hill Education: New York, 2003; Chapter 5, pp 5.0−5.51.
(4) Troitzsch, J. *Plastics Flammability Handbook: Principles, Regulations, Testing, and Approval*; Hanser: Munich, Germany, 2004.
(5) National Research Council (US) Subcommittee on Flame-Retardant Chemicals. *Toxicological Risks of Selected Flame-Retardant Chemicals*; National Academies Press (US): Washington, DC, 2000.
(6) Purser, D. In *Fire Retardant Materials*; Horrocks, A. R., Price, D., Eds.; Woodhead Publishing: Cambridge, UK, 2001; Chapter 3, pp 69−127.
(7) Law, R. J.; Allchin, C. R.; de Boer, J.; Covaci, A.; Herzke, D.; Lepom, P.; Morris, S.; Tronczynski, J.; de Wit, C. A. Levels and Trends of Brominated Flame Retardants in the European Environment. *Chemosphere* **2006**, *64*, 187−208.
(8) Hirschler, M. M. In Handbook of Flame Retardant Textiles; Kilinc, F. S., Ed.; Woodhead Publishing: Cambridge, UK, 2013; Chapter 6, pp 108−173.
(9) Cordner, A.; Mulcahy, M.; Brown, P. Chemical Regulation on Fire: Rapid Policy Advances on Flame Retardants. *Environ. Sci. Technol.* **2013**, *47*, 7067−7076.
(10) Alongi, J.; Horrocks, A. R.; Carosio, F. *Update on Flame Retardant Textiles: State of the Art, Environmental Issues and Innovative Solutions*; Smithers Rapra Technology: Shropshire, UK, 2013.
(11) Morgan, A. B.; Wilkie, C. A. *The Non-halogenated Flame Retardant Handbook*; Wiley: Chichester, UK, 2014.
(12) Bakoš, D.; Košík, M.; Antoš, K.; Karolyová, M.; Vyskočil, I. The Role of Nitrogen in Nitrogen−Phosphorus Synergism. *Fire Mater.* **1982**, *6*, 10−12.
(13) Horrocks, A. R. In *Textile Finishing*; Heywood, D., Ed.; Society of Dyers and Colourists: Bradford, UK, 2003; pp 214−250.
(14) Schindler, W. D.; Hauser, P. J. In *Chemical Finishing of Textiles*; Schindler, W. D., Hauser, P. J., Eds.; Woodhead Publishing: Cambridge, UK, 2003; Chapter 8, pp 98−116.
(15) Castro-Jiménez, J.; Berrojalbiz, N.; Pizarro, M. Dachs, Organophosphate Ester (OPE) Flame Retardants and Plasticizers in the Open Mediterranean and Black Seas Atmosphere. *Environ. Sci. Technol.* **2014**, *48*, 3203−3209.
(16) Salamova, A.; Hermanson, M. H.; Hites, R. A. Organophosphate and Halogenated Flame Retardants in Atmospheric Particles from a European Arctic Site. *Environ. Sci. Technol.* **2014**, *48*, 6133−6140.

DOI: 10.1021/acsami.5b02141
ACS Appl. Mater. Interfaces 2015, 7, 9349−9363

(17) Greaves, A. K.; Letcher, R. J. Metabolites of Organophosphorus Flame Retardants in the Blood Plasma of Herring Gulls from the North American Great Lakes. *Environ. Sci. Technol.* **2014**, *48*, 7942−7950.
(18) Butt, C. M.; Congleton, J.; Hoffman, K.; Fang, M.; Stapleton, H. M. Metabolites of Organophosphate Flame Retardants and 2-Ethylhexyl Tetrabromobenzoate in Urine from Paired Mothers and Toddlers. *Environ. Sci. Technol.* **2014**, *48*, 10432−10438.
(19) Zhang, Q.; Lu, M.; Dong, X.; Wang, C.; Zhang, C.; Liu, W.; Zhao, M. Potential Estrogenic Effects of Phosphorus-containing Flame Retardants. *Environ. Sci. Technol.* **2014**, *48*, 6995−7001.
(20) Laachachi, A.; Ball, V.; Apaydin, K.; Toniazzo, V.; Ruch, D. Diffusion of Polyphosphates into (Poly(allylamine)-Montmorillonite) Multilayer Films: Flame Retardant-Intumescent Films with Improved Oxygen Barrier. *Langmuir* **2011**, *27*, 13879−13887.
(21) Apaydin, K.; Laachachi, A.; Fouquet, T.; Jimenez, M.; Bourbigot, S.; Ruch, D. Mechanistic Investigation of Flame Retardant Coatings made by Layer-by-Layer. *RSC Adv.* **2014**, *4*, 43326−43334.
(22) Li, Y.-C.; Mannen, S.; Morgan, A. B.; Chang, S.; Yang, Y.-H.; Condon, B.; Grunlan, J. C. Intumescent All-P olymer Multilayer Nanocoating Capable of Extinguishing Flame on Fabric. *Adv. Mater.* **2011**, *23*, 3926−3931.
(23) Carosio, F.; Alongi, J.; Malucelli, G. Layer by Layer Ammonium Polyphosphate-based Coatings for Flame Retardancy of Polyester−Cotton Blends. *Carbohydr. Polym.* **2012**, *88*, 1460−1469.
(24) Laufer, G.; Kirkland, C.; Cain, A. A.; Grunlan, J. C. Clay-Chitosan Nanobrick Walls: Completely Renewable Gas Barrier and Flame-retardant Nanocoatings. *ACS Appl. Mater. Interfaces* **2012**, *4*, 1643−1649.
(25) Zhang, T.; Yan, H.; Wang, L.; Fang, Z. Controlled Formation of Self-extinguishing Intumescent Coating on Ramie Fabric via Layer-by-Layer Assembly. *Ind. Eng. Chem. Res.* **2013**, *52*, 6138−6146.
(26) Li, Y.-C.; Schulz, J.; Mannen, S.; Delhom, C.; Condon, B.; Chang, S.; Zammarano, M.; Grunlan, J. C. Flame Retardant Behavior of Polyelectrolyte-Clay Thin Film Assemblies on Cotton Fabric. *ACS Nano* **2010**, *4*, 3325−3337.
(27) Horrocks, A. R.; Nazaré, S.; Masood, R.; Kandola, B.; Price, D. Surface Modification of Fabrics for Improved Flash-fire Resistance using Atmospheric Pressure Plasma in the Presence of a Functionalized Clay and Polysiloxane. *Polym. Adv. Technol.* **2010**, *22*, 22−29.
(28) Gilman, J. W. In *Flame Retardant Polymer Nanocompostites*; Morgan, A. B., Wilkie, C. A., Eds.; Wiley: Hoboken, NJ, 2007; Chapter 3, pp 67−87.
(29) Zhang, T.; Yan, H.; Peng, M.; Wang, L.; Ding, H.; Fang, Z. Construction of Flame Retardant Nanocoating on Ramie Fabric via Layer-by-Layer Assembly of Carbon Nanotube and Ammonium Polyphosphate. *Nanoscale* **2013**, *5*, 3013−3021.
(30) Carosio, F.; Di Blasio, A.; Alongi, J.; Malucelli, G. Green DNA-based Flame Retardant Coatings Assembled through Layer by Layer. *Polymer* **2013**, *54*, 5148−5153.
(31) Alongi, J.; Malucelli, G. State of the Art and Perspectives on Sol−Gel derived Hybrid Architectures for Flame Retardancy of Textiles. *J. Mater. Chem.* **2012**, *22*, 21805−21809.
(32) Brancatelli, G.; Colleoni, C.; Massafra, M. R. Rosace, G. Effect of Hybrid Phosphorus- doped Silica Thin Films produced by Sol-Gel Method on the Thermal Behavior of Cotton Fabrics. *Polym. Degrad. Stab.* **2011**, *96*, 483−490.
(33) Gonçalves, A. G.; Jarrais, B.; Pereira, C.; Morgado, J.; Freire, C.; Pereira, M. F. R. Functionalization of Textiles with Multi-walled Carbon Nanotubes by a Novel Dyeing- like Process. *J. Mater. Sci.* **2012**, *47*, 5263−5275.
(34) Liu, Y.; Wang, X.; Qi, K.; Xin, J. H. Functionalization of Cotton with Carbon Nanotubes. *J. Mater. Chem.* **2008**, *18*, 3454−3460.
(35) Xialing, Wu; Yang, C. Q. Flame Retardant Finishing of Cotton Fleece Fabric: Part III — The Combination of Maleic Acid and Sodium Hypophosphite. *J. Fire Sci.* **2008**, *26*, 351−368.
(36) Blanchard, E. J.; Graves, E. E.; Salame, P. A. Flame Resistant Cotton/Polyester Carpet Materials. *J. Fire Sci.* **2000**, *18*, 151−164.
(37) Wu, X.; Yang, C. Q.; He, Q. Flame Retardant Finishing of Cotton Fleece: Part VII: Polycarboxylic Acids with Different Numbers of Functional Groups. *Cellulose* **2010**, *17*, 859−870.
(38) Cheng, X.; Yang, C. Q. Flame Retardant Finishing of Cotton Fleece Fabric: Part V. Phosphorus-containing Maleic Acid Oligomers. *Fire Mater.* **2009**, *33*, 365−375.
(39) Carosio, F.; Di Blasio, A.; Cuttica, F.; Alongi, J.; Malucelli, G. Flame Retardancy of Polyester and Polyester−Cotton Blends Treated with Caseins. *Ind. Eng. Chem. Res.* **2014**, *53*, 3917−3923.
(40) Opwis, K.; Wego, A.; Bahners, T.; Schollmeyer, E. Permanent Flame Retardant Finishing of Textile Materials by a Photochemical Immobilization of Vinyl Phosphonic Acid. *Polym. Degrad. Stab.* **2011**, *96*, 393−395.
(41) Xing, W.; Jie, G.; Song, L.; Hu, S.; Lv, X.; Wang, X.; Hu, Y. Flame Retardancy and Thermal Degradation of Cotton Textiles based on UV-curable Flame Retardant Coatings. *Thermochim. Acta* **2011**, *513*, 75−82.
(42) Yuan, H.; Xing, W.; Zhang, P.; Song, L.; Hu, Y. Functionalization of Cotton with UV- cured Flame Retardant Coatings. *Ind. Eng. Chem. Res.* **2012**, *51*, 5394−5401.
(43) Tsafack, M. J.; Levalois-Grützmacher, J. Towards Multifunctional Surfaces using the Plasma-induced Graft-polymerization (PIGP) Process: Flame and Waterproof Cotton Textiles. *Surf. Coat. Technol.* **2007**, *201*, 5789−5795.
(44) Çakmakçı, E.; Mülazim, Y.; Kahraman, M. V.; Apohan, N. K. Flame Retardant Thiol-ene Photocured Coatings. *React. Funct. Polym.* **2011**, *71*, 36−41.
(45) Horrocks, A. R. Flame Retardant Challenges for Textiles and Fibres: New Chemistry versus Innovatory Solutions. *Polym. Degrad. Stab.* **2011**, *96*, 377−392.
(46) Horrocks, A. R.; Kandola, B. K.; Davies, P. J.; Zhang, S.; Padbury, S. A. Developments in Flame Retardant Textiles − a Review. *Polym. Degrad. Stab.* **2005**, *88*, 3−12.
(47) Allcock, H. R. Recent Developments in Polyphosphazene Materials Science. *Curr. Opin. Solid State Mater. Sci.* **2006**, *10*, 231−240.
(48) Gleria, M.; De Jaeger, R. Polyphosphazenes: A Review. *Top. Curr. Chem.* **2005**, *250*, 165−251.
(49) Allen, C. W.; Hernandez-Rubio, D. In *Applicative Aspects of Poly(organophosphazenes)*; De Jaeger, R., Gleria, M., Eds.; Nova Science Publishers: Hauppauge, NY, 2004; Chapter 6, pp 119−137.
(50) De Jaeger, R.; Gleria, M. *Applicative Aspects of Poly(organophosphazenes)*; Nova Science Publishers: Hauppauge, NY, 2004.
(51) Huang, X.; Huang, X.-J.; Yu, A.-G.; Wang, C.; Dai, Z.-W.; Xu, Z.-K. Click Chemistry" as a Facile Approach to the Synthesis of Polyphosphazene Glycopolymers. *Macromol. Chem. Phys.* **2010**, *212*, 272−277.
(52) Deng, M.; Kumbar, S. G.; Wan, Y.; Toti, U. S.; Allcock, H. R.; Laurencin, C. T. Polyphosphazene Polymers for Tissue Engineering: An Analysis of Material Synthesis, Characterization and Applications. *Soft Matter* **2010**, *6*, 3119−3132.
(53) Shukla, L.; Arya, P. Flame Retardant based on Poly (Flourophosphanzene) and Organo Brominated Compound for the Polyester/Cotton Shirting. *Text. Dyer Printer* **1998**, *31*, 16−18.
(54) Fukuoka, J.; Iguchi, Y. Fireproofing Finishes for Cellulose Fibers. JP04002881A, January 7, 1992.
(55) Saxena, A. K.; Nigam, V.; Kumar, S.; Kerketta, A. Flame Retardant Composition, Fibers, Processing and Applications of Flame Retardant Composition. WO2014045308A1, March 27, 2014.
(56) Sasakura, T.; Ueda, T. Method and Agents for Finishing Cellulosic Fabrics. JP02289175A, November 29, 1990.
(57) Tsujimoto, H.; Ishikuro, S.; Yonezawa, T.; Watanuki, T. Aminophosphazene-based Fireproofing Agents for Cellulosic Fibers, their Manufacture and Treated Fabric Products. JP2000017574A, January 18, 2000.
(58) Levchik, G. F.; Grigoriev, Y. V.; Balabanovich, A. I.; Levchik, S. V.; Klatt, M. Phosphorus-nitrogen Containing Fire Retardants for Poly(butylene terephthalate). *Polym. Int.* **2000**, *49*, 1095−1100.

DOI: 10.1021/acsami.5b02141
ACS Appl. Mater. Interfaces 2015, 7, 9349−9363

(59) Levchik, S. V.; Levchik, G. F.; Balabanovich, A. I.; Weil, E. D.; Klatt, M. Phosphorus Oxynitride: A Thermally Stable Fire Retardant Additive for Polyamide 6 and Poly(butylene terephthalate). *Angew. Makromol. Chem.* **1999**, *264*, 48−55.
(60) Allen, C. W. The Use of Phosphazenes as Fire Resistant Materials. *J. Fire Sci.* **1993**, *11*, 320−328.
(61) Sun, J.; Wang, X.; Wu, D. Novel Spirocyclic Phosphazene-Based Epoxy Resin for Halogen-Free Fire Resistance: Synthesis, Curing Behaviors, and Flammability Characteristics. *ACS Appl. Mater. Interfaces* **2012**, *4*, 4047−4061.
(62) Zhang, X.; Zhong, Y.; Mao, Z.-P. The flame Retardancy and Thermal Stability Properties of Poly (ethylene terephthalate)/Hexakis (4-nitrophenoxy) cyclotriphosphazene Systems. *Polym. Degrad. Stab.* **2012**, *97*, 1504−1510.
(63) Praschak, D.; Bahners, T.; Schollmeyer, E. Excimer UV Lamp Irradiation induced Grafting on Synthetic Polymers. *Appl. Phys. A: Mater. Sci. Process* **2000**, *71*, 577−581.
(64) Opwis, K.; Bahners, T.; Schollmeyer, E. Improvement of the Alkali-resistance of Poly(ethylene terephthalate) by a Photo-chemical Modification using Excimer-UV-Lamps. *Chem. Fibers Int.* **2004**, *54*, 116−119.
(65) Gao, S. L.; Häßler, R.; Mäder, E.; Bahners, T.; Opwis, K.; Schollmeyer, E. Photochemical Surface Modification of PET by Excimer UV Lamp Irradiation. *Appl. Phys. B: Lasers Opt.* **2005**, *81*, 681−690.
(66) Allcock, H. R. *Chemistry and Applications of Polyphosphazenes*; Wiley: Hoboken, NJ, 2003.
(67) Mujumdar, A. N.; Young, S. G.; Merker, R. L.; Magill, J. H. A Study of Solution Polymerization of Polyphosphazenes. *Macromolecules* **1990**, *23*, 14−21.
(68) Imada, A. Resin Composition and Resin molded Product. US2014/0114028Al.
(69) Jain, R. K.; Lal, K.; Bhatnagar, H. L. Thermal Degradation of Cellulose and its Phosphorylated Products in Air and Nitrogen. *J. Appl. Polym. Sci.* **1985**, *30*, 897−914.
(70) Steger, E. Zur Konstitution des Phosphams und verwandter Verbindungen auf Grund der Infrarotspektren. *Chem. Ber.* **1961**, *94*, 266−272.

DOI: 10.1021/acsami.5b02141
ACS Appl. Mater. Interfaces 2015, 7, 9349−9363